JOURNAL OF GUIDANCE, CONTROL, AND DYNAMICS
Vol. 18, No. 6, November–December 1995

Fuel/Time Optimal Control of the Benchmark Problem

Tarunraj Singh*
State University of New York at Buffalo, Buffalo, New York 14260

Design of fuel/time optimal control of the benchmark two-mass/spring system is addressed in the frequency domain. The optimal control profile is represented as the output of a time-delay filter, where the amplitude of the time-delayed signals are constrainted to satisfy the control bounds. The time delays of the filter are determined by solving a parameter optimization problem that minimizes a weighted fuel/time cost function subject to the constraint that the time-delay filter cancel all the poles of the system and the control profile satisfies the rigid-body boundary conditions. It is shown that three control structures exist: a three-switch profile corresponding to the time optimal control problem that changes to a six-switch profile corresponding to a cost function that includes a small weight on the fuel. As the weight on the fuel increases beyond a critical value, the control profile changes to a two-switch profile. The value of the critical weight that represents the transition of the control profile from a six-switch to a two-switch control profile is determined.

I. Introduction

OPTIMAL control of flexible structures has been addressed by numerous researchers. The cost functions to be optimized have included maneuver time,[1–4] quadratic cost functions of state and control,[5] fuel used,[6] residual structural energy,[7] variation of boundary conditions to system parameters,[8] etc. Design of controllers that optimize a weighted fuel/time cost function has received considerably less attention. Vander Velde and He[9] proposed a technique to approximate the control profile that minimized a weighted combination of the maneuver time and fuel consumed for flexible space structures. Because of its approximate nature, residual vibrations are unavoidable. Souza[10] solved the weighted fuel/time problem for an undamped harmonic oscillator exactly for any initial conditions. Deriving the exact solution for the weighed fuel/time problem is attractive since it includes, in the limit, the time optimal and fuel optimal cases.

This paper addresses the problem of design of a fuel/time optimal controller for a two-mass/spring system that is representative of a dynamic system with noncollocated sensor–actuator pair. This problem, proposed by Wie and Bernstein,[11] is representative of many flexible structures, whose response is characterized by one rigid-body mode and one vibration mode. The design of a fuel/time optimal controller is posed as the design of a time-delay filter that generates a bang–off-bang profile when it is subject to a step input. The magnitudes of the time-delayed signals are constrained to satisfy the saturation limits of the actuator. Closed-form solutions of the times delays as functions of the weighting parameter and the net rigid-body motion are derived for the large-α (weighting parameter) case. The optimization problem results in an integer programming problem that uniquely determines the optimal control profile. This paper also shows that, for a cost function with a very small weighting parameter associated with the fuel, the optimal control profile is a sequence of pulses characterized by six switches. As the weighting parameter increases, the optimal control profile approaches the well-known structure of a fuel optimal control profile characterized by two switches.

This paper begins with the determination of the closed-form solution of the two-switch bang–off-bang optimal control profile. One of the limiting control profiles for the generic fuel/time optimal controller is the time optimal profile, which has a three-switch bang–bang structure. Since the two-switch control profile cannot generate a three-switch bang–bang profile, there should exist a six-switch control profile that can, in the limit, lead to the three-switch bang–bang and the two-switch bang–off-bang control profile. The next section of this paper determines the value of the weighting parameter that corresponds to the transition of the six-switch-to-two-switch control profile. The paper concludes with a section that summarizes the results.

II. Statement of Problem

Fuel/time optimal control design of a linear system

$$\dot{x} = Ax + Bu \tag{1}$$

where $x \in \Re^n$ and

$$-1 \le u \le 1 \tag{2}$$

where $u \in \Re$, leads to a control input that minimizes

$$J = \int_0^{t_f} (1 + \alpha|u|)\, dt \tag{3}$$

where the cost function J is a weighted ($\alpha > 0$) combination of the maneuver time and fuel consumed. Define the Hamiltonian as

$$H(x, \lambda, u) = 1 + \alpha|u| + \lambda^T(Ax + Bu) \tag{4}$$

where λ is the costate vector. The necessary conditions for optimality require the following equations to be satisfied:

$$\dot{x} = Ax + Bu \qquad \forall t \in [0, t_f] \tag{5}$$

$$\dot{\lambda} = -A^T\lambda \qquad \forall t \in [0, t_f] \tag{6}$$

$$u = -\mathrm{dez}\left(\frac{B^T\lambda}{\alpha}\right) \qquad \forall t \in [0, t_f] \tag{7}$$

which is prescribed by Pontryagin's minimum principle and

$$H(x, \lambda, u) = 1 + \alpha|u| + \lambda^T(Ax + Bu) = 0 \qquad \forall t \in [0, t_f] \tag{8}$$

in addition to the boundary conditions

$$x(0) = 0, \qquad x(t_f) = \text{prescribed} \tag{9}$$

The dead-zone function dez is defined as

$$\phi = \mathrm{dez}(\psi) \Rightarrow \begin{cases} \phi = 0 & \text{if } |\psi| < 1 \\ \phi = \mathrm{sgn}(\psi) & \text{if } |\psi| > 1 \\ 0 \le \phi \le 1 & \text{if } \psi = 1 \\ -1 \le \phi \le 0 & \text{if } \psi = -1 \end{cases} \tag{10}$$

Received May 7, 1994; revision received Dec. 23, 1994; accepted for publication June 1, 1995.

*Assistant Professor, Mechanical and Aerospace Engineering. Member AIAA.

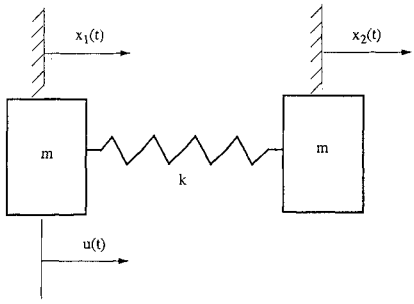

Fig. 1 Two-mass–spring system.

III. Problem Formulation

The equations of motion of a two-mass–spring system (Fig. 1) are

$$\begin{aligned} m\ddot{x}_1 + k(x_1 - x_2) &= u \\ m\ddot{x}_2 - k(x_1 - x_2) &= 0 \end{aligned} \tag{11}$$

where x_1 and x_2 represent the displacement of the first and second mass, respectively. The eigenvector matrix Φ can be used to decouple the equations of motion to the form

$$\begin{aligned} \ddot{\theta} &= \phi_0 u \\ \ddot{q} + \omega^2 q &= \phi_1 u \end{aligned} \tag{12}$$

where

$$\begin{bmatrix} \phi_0 \\ \phi_1 \end{bmatrix} = \Phi^T \begin{bmatrix} 1 \\ 0 \end{bmatrix} \tag{13}$$

The variable θ will be referred to as the rigid-body mode and q as the vibratory mode characterized by a frequency ω.

The objective of minimizing a cost function, which is a weighted combination of the maneuver time and the fuel consumed, is achieved by the design of the transfer function of a time-delay filter, a set of zeros of which are constrained to cancel the poles of the system. Additional constraints including actuator limits and boundary conditions are included in the design process. We assume $m = 1$ and $k = 1$ for the generation of numerical results in this work.

IV. Control Parametrization

With the knowledge that the fuel/time optimal control profile is bang–off-bang (proof of the preclusion of singularity intervals is included in the appendix), we construct a time-delay filter whose output is bang–off-bang when it is subject to a step input. The amplitudes of the time-delayed signals are constrainted by the bounds on the control, requiring the determination of the time delays to completely specify the time-delay filter.

To define the time-delay filter completely, one can formulate a constrainted parameter optimization problem, where the parameters to be determined are the time delays. To eliminate any residual vibration of the system, the complex poles located at $\pm j\omega$ have to be canceled by a complex conjugate pair of zeros of the time-delay filter leading to the first constraint. The next constraint to satisfy the boundary conditions is arrived at by integrating the rigid-body equation of motion. Singh and Vadali[2] have illustrated that the transfer function of a time-delay filter that generates a control profile that is antisymmetric about its midmaneuver time has a minimum of two zeros at the origin of the complex plane, which cancel the rigid-body poles of the system. This fact is exploited to reduce the dimension of the parameter search space.

We consider the problem of reorientation, i.e., a rest-to-rest maneuver with boundary conditions

$$\begin{aligned} x_1(0) = x_2(0) = 0, \qquad & x_1(t_f) = x_2(t_f) = \theta_f/2\phi_0 \\ \dot{x}_1(0) = \dot{x}_2(0) = 0, \qquad & \dot{x}_1(t_f) = \dot{x}_2(t_f) = 0 \end{aligned} \tag{14}$$

which corresponds to

$$\begin{aligned} \theta(0) = q(0) = 0, \qquad & \theta(t_f) = \theta_f, \qquad q(t_f) = 0 \\ \dot{\theta}(0) = \dot{q}(0) = 0, \qquad & \dot{\theta}(t_f) = \dot{q}(t_f) = 0 \end{aligned} \tag{15}$$

in the decoupled state space. The two-switch control profile for a fuel/time optimal (Fig. 2) problem is parametrized in frequency domain as

$$u = (1/s)\left(1 - e^{-s(T_2 - T_1)} - e^{-s(T_2 + T_1)} + e^{-2sT_2}\right) \tag{16}$$

where T_2 is the midmaneuver time and $T_2 - T_1$ is the first switch time. The transfer function of the time-delay filter that generates the bang–off-bang control profile is

$$G(s) = \left(1 - e^{-s(T_2 - T_1)} - e^{-s(T_2 + T_1)} + e^{-2sT_2}\right) \tag{17}$$

From the Laplace transform of the decoupled rigid-body mode [Eq. (12)], we have

$$s^2\theta(s) = (\phi_0/s)\left(1 - e^{-s(T_2 - T_1)} - e^{-s(T_2 + T_1)} + e^{-2sT_2}\right) \tag{18}$$

The inverse Laplace transform leads to

$$\begin{aligned} \theta(t) = \phi_0\Big(&\tfrac{1}{2}t^2 - \mathcal{H}[t - (T_2 - T_1)]\left\{\tfrac{1}{2}[t - (T_2 - T_1)]^2\right\} \\ &- \mathcal{H}[t - (T_2 + T_1)]\left\{\tfrac{1}{2}[t - (T_2 + T_1)]^2\right\} \\ &- \mathcal{H}(t - 2T_2)\left[\tfrac{1}{2}[t - 2T_2)^2\right]\Big) \end{aligned} \tag{19}$$

where $\mathcal{H}(t - T_i)$ is the Heaviside unit function. The final state of θ is $\theta(2T_2) = \theta_f$, which leads to

$$\theta_f = \phi_0\left(T_2^2 - T_1^2\right) \tag{20}$$

which can be rewritten as

$$(\theta_f/\phi_0) = (T_2 - T_1)(T_2 + T_1) \tag{21}$$

To cancel the vibration mode, we substitute $s = j\omega$ into Eq. (17), and equating the real and imaginary parts to zero, we have

$$1 - \cos[\omega(T_2 - T_1)] - \cos[\omega(T_2 + T_1)] + \cos(2\omega T_2) = 0 \tag{22}$$

$$-\sin[\omega(T_2 - T_1)] - \sin[\omega(T_2 + T_1)] + \sin(2\omega T_2) = 0 \tag{23}$$

respectively. Equations (22) and (23) can be simplified to

$$2\cos(\omega T_2)[-\cos(\omega T_1) + \cos(\omega T_2)] = 0 \tag{24}$$

$$2\sin(\omega T_2)[-\cos(\omega T_1) + \cos(\omega T_2)] = 0 \tag{25}$$

respectively, leading to the constraint equation

$$-\cos(\omega T_1) + \cos(\omega T_2) = 0 \tag{26}$$

Solving Eq. (26), we have

$$\omega T_2 = \pm\omega T_1 + 2n\pi \qquad n = \pm 1, \pm 2, \ldots, \pm\infty \tag{27}$$

Substituting Eq. (27) in Eq. (21), we have

$$T_1 = \begin{cases} \dfrac{\omega\theta_f}{4n\pi\phi_0} - \dfrac{n\pi}{\omega} & \text{for } \omega T_2 = \omega T_1 + 2n\pi \\ \dfrac{n\pi}{\omega} - \dfrac{\omega\theta_f}{4n\pi\phi_0} & \text{for } \omega T_2 = -\omega T_1 + 2n\pi \end{cases} \tag{28}$$

The next step includes determining the integer n. The cost function to be minimized is

$$J = \int_0^{2T_2} (1 + \alpha|u|)\, dt \tag{29}$$

which can be rewritten as

$$J = 2T_2 + 2\alpha(T_2 - T_1) \tag{30}$$

or

$$J = \begin{cases} \dfrac{\omega\theta_f}{2n\pi\phi_0} + (2 + 4\alpha)\dfrac{n\pi}{\omega} & \text{for } \omega T_2 = \omega T_1 + 2n\pi \\ (1 + 2\alpha)\dfrac{\omega\theta_f}{2n\pi\phi_0} + \dfrac{2n\pi}{\omega} & \text{for } \omega T_2 = -\omega T_1 + 2n\pi \end{cases} \tag{31}$$

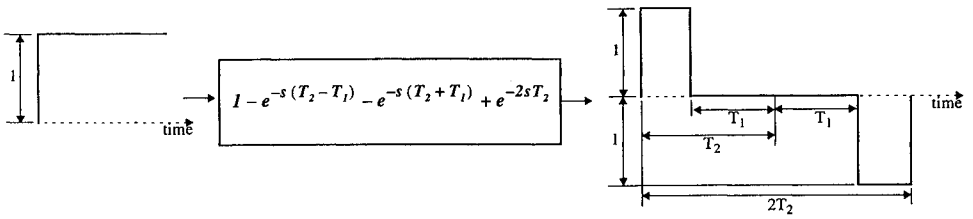

Fig. 2 Time-delay filter.

Since the cost J is a unimodal function for positive n (negative n are not valid as they imply a negative cost J), we can solve for n_{opt} that minimizes J, assuming n is continuous. The integer values that flank n_{opt} are used to determine the optimum n. Assuming n is continuous, we require

$$\frac{dJ}{dn} = 0 \tag{32}$$

for optimality, which leads to

$$n^2 = \begin{cases} \left(\dfrac{\omega}{\pi}\right)^2 \dfrac{\theta_f}{(2+4\alpha)\phi_0} & \text{for } \omega T_2 = \omega T_1 + 2n\pi \\ \left(\dfrac{\omega}{\pi}\right)^2 \dfrac{(1+2\alpha)\theta_f}{2\phi_0} & \text{for } \omega T_2 = -\omega T_1 + 2n\pi \end{cases} \tag{33}$$

Since n is an integer, the value of J corresponding to the integer values of n that flank the value of n estimated by Eq. (33) are evaluated to determine the optimum n. A point to note is that the optimal control profile leads to displacement of the rigid-body mode at midmaneuver time, which is half the total maneuver, and the displacement of the vibratory mode, which is zero at the midmaneuver time.

To compare the solution of the spring–mass system to a rigid-body system with the same mass as the spring–mass system, we arrive at a closed-form solution of the fuel/time optimum control profile for a rigid body that has the same structure as the two-mass–spring system. The system in question is

$$\ddot{\theta} = \phi_0 u \tag{34}$$

The control profile parametrized in terms of the switch times and the final time is

$$u = (1/s)\left(1 - e^{-s(T_2-T_1)} - e^{-s(T_2+T_1)} + e^{-2sT_2}\right) \tag{35}$$

The boundary constraint leads to

$$T_2^2 = (\theta_f/\phi_0) + T_1^2 \tag{36}$$

Substituting Eq. (36) into Eq. (29), we have

$$J = 2(\alpha+1)\sqrt{(\theta_f/\phi_0) + T_1^2} - 2\alpha T_1 \tag{37}$$

The parameter T_1 that optimizes the cost function is given by the equation

$$\frac{dJ}{dT_1} = 0 \tag{38}$$

which leads to

$$T_1^2 = \frac{\alpha^2\theta_f}{(1+2\alpha)\phi_0} \tag{39}$$

Substituting Eq. (39) into Eq. (37), we have

$$J = 2\sqrt{\theta_f(1+2\alpha)/\phi_0} \tag{40}$$

Figure 3 illustrates the cost function for different values of n. The highlighted portion of the graph exemplifies the variation of the optimum cost as a function of α for the benchmark problem. The highlighted portion of the graph is tangential to the graph of the cost function for the rigid-body case for discrete values of α.

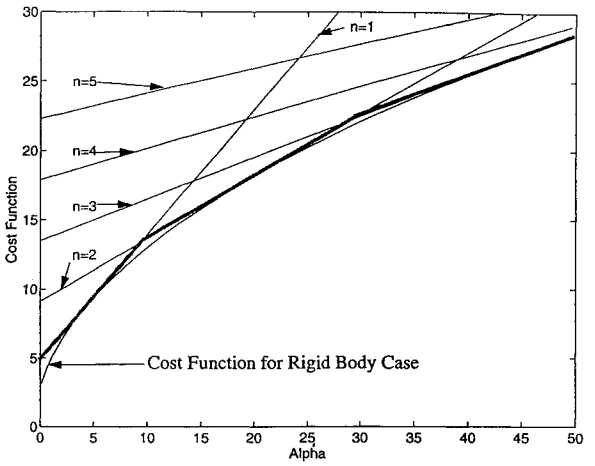

Fig. 3 Cost variation as function of α.

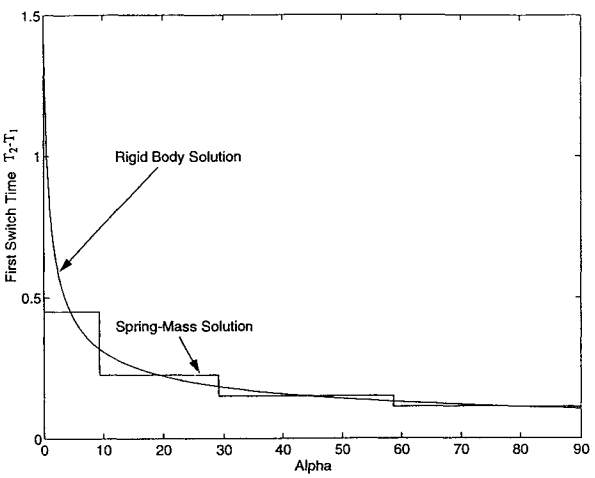

Fig. 4 First switch time vs α.

Since n is a constant for a specific range of α, T_1 and T_2 are constant in the same interval. This implies that the optimum control is identical for different values of α. Plotting the first switch time and the maneuver time of the optimal controller for a spring–mass system and a rigid body of the same mass as the spring–mass system (Figs. 4 and 5), we see that, for certain values of α, the maneuver time of the spring–mass case is smaller than the rigid case. However, the cost function of the spring–mass case is always greater than or equal to that of the rigid case. For $\alpha = 0$, which corresponds to the time optimal case, the first switch time coincides with the midmaneuver time for the rigid-body case, leading to a control profile that is bang–bang.

Equation (33) indicates two possible solutions that are functions of θ_f and α. Plotting the cost function versus θ_f and α (Fig. 6), we see that, for small θ_f, the solution corresponding to $\omega T_2 = -\omega T_1 + 2n\pi$ (case 2) is optimum, whereas for large values of θ_f, $\omega T_2 = \omega T_1 + 2n\pi$ (case 1) leads to the optimum solution. This results from the slope of the optimum cost curve as a function of θ_f being smaller for case 1, as indicated by Eq. (31), for any α greater than 0.

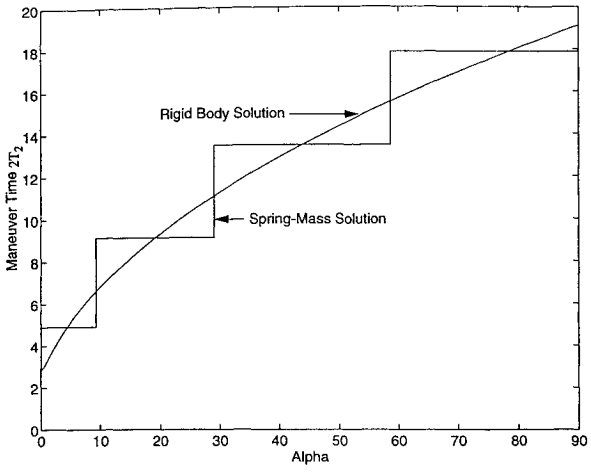

Fig. 5 Maneuver time vs α.

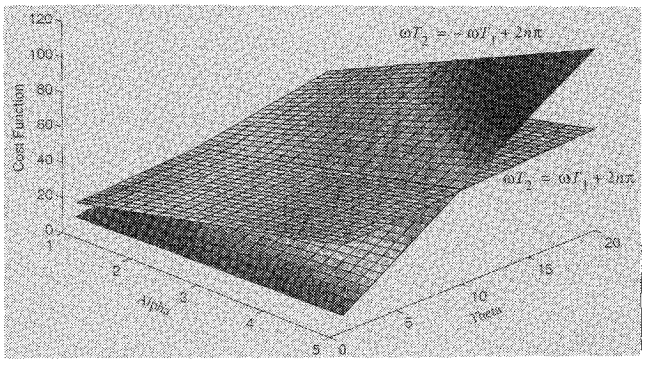

Fig. 6 Cost function vs α and maneuver θ_f.

V. Small α Control Profile

Singh and Vadali[2] have shown that the control profile corresponding to $\alpha = 0$, i.e., the time optimal control profile, has a three-switch bang–bang structure (Fig. 7), which is antisymmetric about its midmaneuver time. The structure of this control profile is radically different from the control profile parametrized to optimize the weighted fuel/time cost function. This leads us to conjecture that there should exist a control structure that in the limit can generate the time optimal control profile and the control structure discussed in Sec. IV. The control profile illustrated in Fig. 8, which is antisymmetric about the midmaneuver time, satisfies this objective.

For $\alpha = 0$, $T_1 = 0$ and $T_2 = T_3$, resulting in the time optimal control structure (Fig. 7). For $\alpha > \alpha_{cr}$, the switch times $T_1 = T_2$, generating the control profile of Fig. 2. Here, α_{cr} is the critical value of α at which the structure of the control profile changes from that of Fig. 8 to that represented in Fig. 2.

The antisymmetric fuel/time optimal control profile for small α is parametrized as

$$u = (1/s)\left(1 - e^{-s(T_4-T_3)} - e^{-s(T_4-T_2)} + e^{-s(T_4-T_1)} + e^{-s(T_4+T_1)} - e^{-s(T_4+T_2)} - e^{-s(T_4-T_3)} + e^{-2sT_4}\right) \tag{41}$$

where T_4 is the midmaneuver time. As in Sec. IV, the constraints for the parameter optimization problem can be shown to be

$$\theta_f = \phi_0\left(T_4^2 - T_3^2 + T_2^2 - T_1^2\right) \tag{42}$$

which is derived from the rigid-body boundary condition, and

$$-\cos(\omega T_3) + \cos(\omega T_2) - \cos(\omega T_1) + \cos(\omega T_4) = 0 \tag{43}$$

which forces the transfer function of the time-delay filter to cancel the frequency corresponding to the vibratory mode of the system.

A parameter optimization problem is formulated to solve for the time delays. The cost function to be minimized is

$$J = \int_0^{t_f} (1 + \alpha|u|)\,dt = 2T_4 + 2\alpha[(T_4 - T_3) + (T_2 - T_1)] \tag{44}$$

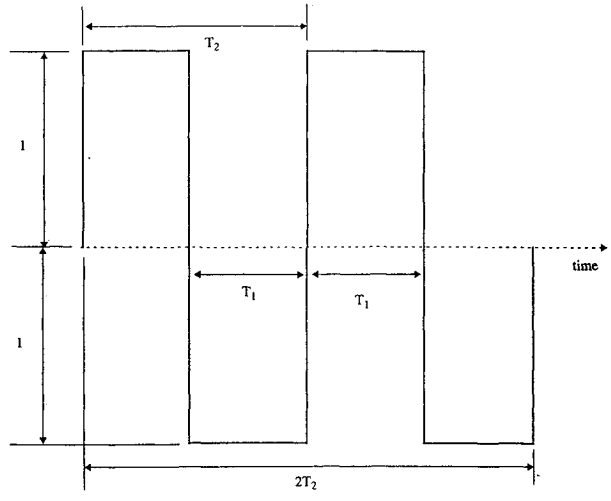

Fig. 7 Bang–bang control profile.

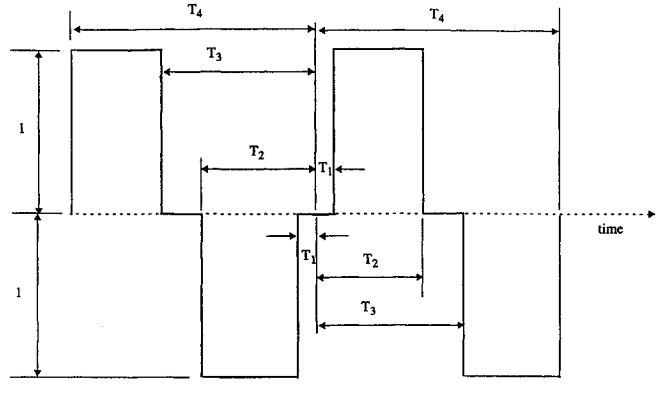

Fig. 8 Transition control profile.

subject to constraints given by Eqs. (42) and (43). Since the constraints are nonlinear and there are more parameters than constraints, there exist a potential for the existence of multiple solutions. To prove optimality of the control profile, the control profile predicted by the switching function should coincide with that predicted by the parameter optimization. To determine the switching function, we need to solve for the initial costates. We know that

$$\lambda(t) = \exp(-A^T t)\lambda(0) \tag{45}$$

We also know that the switching function has to satisfy

$$\begin{bmatrix} B^T \exp\left[-A^T(T_4 - T_3)\right] \\ B^T \exp\left[-A^T(T_4 - T_2)\right] \\ B^T \exp\left[-A^T(T_4 + T_2)\right] \\ B^T \exp\left[-A^T(T_4 + T_3)\right] \end{bmatrix} \lambda(0) = \begin{Bmatrix} -\alpha \\ \alpha \\ -\alpha \\ \alpha \end{Bmatrix} \tag{46}$$

Solving for $\lambda(0)$ from Eq. (46) and substituting in

$$u = -\text{dez}[B^T \exp(-A^T t)\lambda(0)/\alpha] \tag{47}$$

we can arrive at the control profile that should coincide with the one predicted by the parametrization problem for optimality.

VI. Determination of α_{cr}

The vector differential equation representing the equations of motion of the two-mass–spring system is

$$\dot{x} = Ax + Bu \qquad |u| \le 1 \tag{48}$$

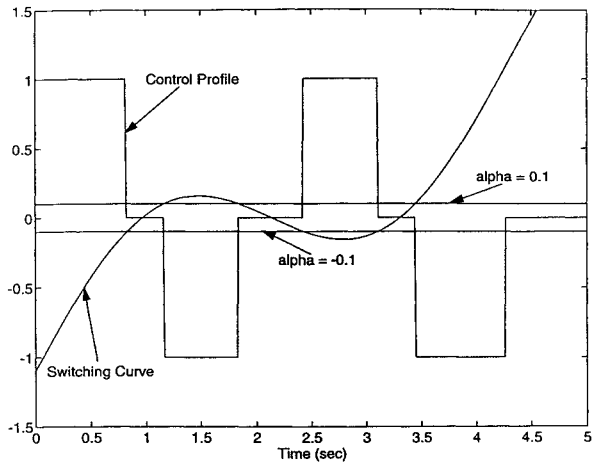

Fig. 9 Switching function and corresponding control profile.

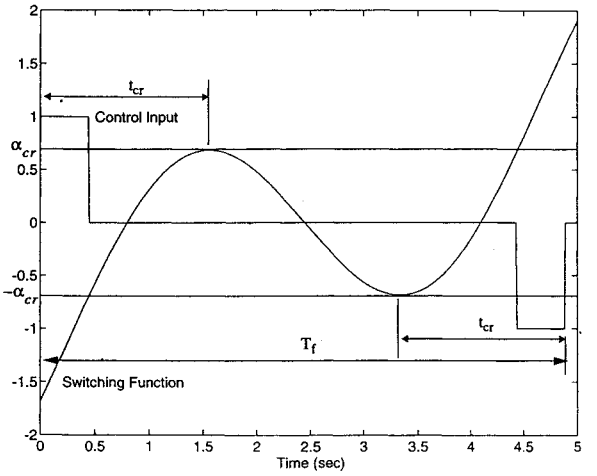

Fig. 10 Large α control profile.

where $x \in \Re^4$, u is a scalar, and the matrices A and B are given by

$$A = \begin{bmatrix} 0 & 1 & 0 & 0 \\ 0 & 0 & 0 & 0 \\ 0 & 0 & 0 & 1 \\ 0 & 0 & -\omega^2 & 0 \end{bmatrix} \tag{49}$$

$$B = \begin{bmatrix} 0 \\ \phi_0 \\ 0 \\ \phi_1 \end{bmatrix} \tag{50}$$

respectively. The optimal control is given by

$$u(t) = -\text{dez}[B^T\lambda(t)/\alpha] \tag{51}$$

where $\lambda(t)$ is the costate vector, which is given by the equation

$$\lambda(t) = \exp(-A^T t)\lambda(0) \tag{52}$$

We know that the control structure of Fig. 8 is generated by the switching function $B^T\lambda(t)$ shown in Fig. 9.

Here, α_{cr} corresponds to the α when the switching function $B^T\lambda(t)$ equals a value of α and $-\alpha$ at times t_{cr} and $T_f - t_{cr}$, respectively (Fig. 10), i.e.,

$$B^T\lambda(t_{cr}) = B^T\exp\left(-A^T t_{cr}\right)\lambda(0) = \alpha_{cr} \tag{53}$$

$$B^T\lambda(T_f - t_{cr}) = B^T\exp\left[-A^T(T_f - t_{cr})\right]\lambda(0) = -\alpha_{cr} \tag{54}$$

and to ensure that the switching function touches the lines parallel to the abscissa with ordinate intercepts of $\pm\alpha_{cr}$, tangentially, we require the slope of $B^T\lambda(t)$ at t_{cr} and $T_f - t_{cr}$ be equal to zero (Fig. 10), i.e.,

$$\frac{d}{dt}[B^T\lambda(t)]\bigg|_{t=t_{cr}} = -B^T A^T\exp\left(-A^T t_{cr}\right)\lambda(0) = 0 \tag{55}$$

$$\frac{d}{dt}[B^T\lambda(t)]\bigg|_{t=t_{cr}} = -B^T A^T\exp\left[-A^T(T_f - t_{cr})\right]\lambda(0) = 0 \tag{56}$$

Solving Eqs. (53–56), which are rewritten as

$$\begin{bmatrix} B^T\exp\left(-A^T t_{cr}\right) \\ B^T\exp\left[-A^T(T_f - t_{cr})\right] \\ -B^T A^T\exp\left(-A^T t_{cr}\right) \\ -B^T A^T\exp\left[-A^T(T_f - t_{cr})\right] \end{bmatrix}\lambda(0) = \begin{Bmatrix} \alpha_{cr} \\ -\alpha_{cr} \\ 0 \\ 0 \end{Bmatrix} \tag{57}$$

we arrive at t_{cr} and α_{cr}. To determine $\lambda(0)$, we consider the following equations:

$$B^T\exp\left[-A^T(T_2 - T_1)\right]\lambda(0) = -\alpha \tag{58}$$

$$B^T\exp\left[-A^T(T_2 + T_1)\right]\lambda(0) = \alpha \tag{59}$$

which are satisfied at the switch times $T_2 - T_1$ and $T_2 + T_1$, respectively; the switching function evaluated at time T_2

$$B^T\exp\left(-A^T T_2\right)\lambda(0) = 0 \tag{60}$$

which is proven in the Appendix; and

$$B^T\lambda(0) = -1 - \alpha \tag{61}$$

which is derived from the Hamiltonian evaluated at time = zero.

Figures 4 and 5 indicate that the switch times T_1 and T_2 remain constant for small α, i.e., for the range of α greater than α_{cr} and less than $\alpha = 9.87$ (for a maneuver of $\theta_f = 1$). Equations (58–61) can now be represented as

$$P\lambda(0) = \begin{Bmatrix} -\alpha \\ \alpha \\ 0 \\ -1 - \alpha \end{Bmatrix} \tag{62}$$

where

$$P = \begin{bmatrix} B^T\exp\left[-A^T(T_2 - T_1)\right] \\ B^T\exp\left[-A^T(T_2 + T_1)\right] \\ B^T\exp\left(-A^T T_2\right) \\ B^T \end{bmatrix} \tag{63}$$

Since T_1 and T_2 are constant for α greater than α_{cr} and less than 9.87, P is a constant matrix. Thus, α_{cr} and t_{cr} are solved from the equation

$$\begin{bmatrix} B^T\exp\left(-A^T t_{cr}\right)P^{-1} \\ B^T\exp\left[-A^T(T_f - t_{cr})\right]P^{-1} \\ -B^T A^T\exp\left(-A^T t_{cr}\right)P^{-1} \\ -B^T A^T\exp\left[-A^T(T_f - t_{cr})\right]P^{-1} \end{bmatrix}\begin{Bmatrix} -\alpha_{cr} \\ \alpha_{cr} \\ 0 \\ -1 - \alpha_{cr} \end{Bmatrix} = \begin{Bmatrix} \alpha_{cr} \\ -\alpha_{cr} \\ 0 \\ 0 \end{Bmatrix} \tag{64}$$

For $\theta_f = 1$, the solution is $\alpha_{cr} = 0.6824$.

To study the effect of the frequency of the vibratory mode on α_{cr} and the transition switch point, the procedure delineated above is used to generate Figs. 11 and 12 for a maneuver $\theta_f = 1$. With the masses being fixed, the frequency of the vibratory mode is proportional to the stiffness. Hence, we study the effect of stiffness on α_{cr}

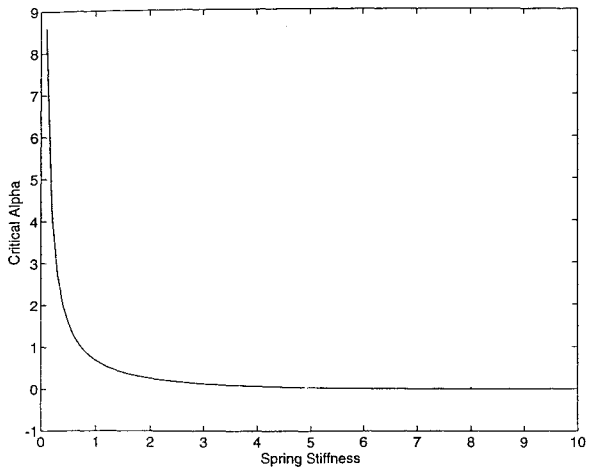

Fig. 11 Variation of α_{cr} vs spring stiffness.

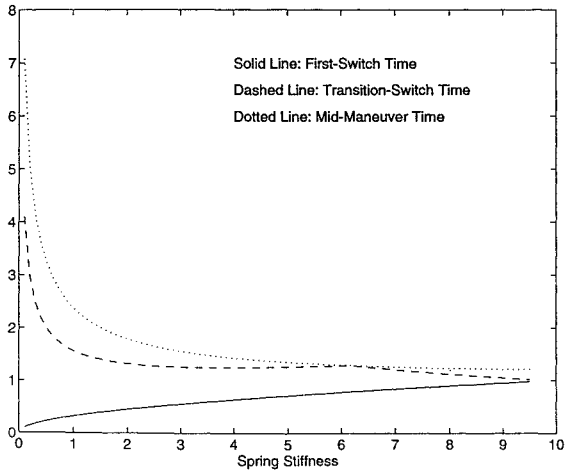

Fig. 12 Variation of transition switch point t_{cr} vs spring stiffness.

and the transition switch point. Figure 11 reveals that α_{cr} tends to zero as the stiffness increases and increases rapidly as the stiffness tends to zero.

Figure 12 illustrates the variation of the transition switch point in correspondence with the first switch time and the midmaneuver time. It is seen that the transition switch time lies between the first switch time curve and the midmaneuver time, which asymptotically approach each other. This makes intuitive sense, since the system is approaching a rigid body as the stiffness increases, and with the knowledge that α_{cr} tends to zero as the stiffness increases, the control profile should resemble a bang–bang controller for a rigid body.

VII. Conclusions

A frequency-domain approach to the design of fuel/time optimal control is proposed and illustrated on the benchmark two-mass/spring system. The exact solution to the fuel/time optimal controller, which is a two-switch bang–off-bang control profile, is derived for large α. The discontinuous nature of the variation of the switch time and maneuver time as a function of the weighting parameter is illustrated. It is shown that the control profile for the benchmark problem is exactly the same as that for the rigid-body case for specific values of α. The presence of a six-switch bang–off-bang profile for small α is proposed and the value of α corresponding to the transition from the six-switch to the two-switch bang–off-bang profile is evaluated for a specific maneuver.

Appendix

Two results regarding the existence of singular intervals and evolution of the switching function are derived. The first result precludes the existence of singular intervals and the second result indicates that the switching function is equal to zero at the midmaneuver time.

The fuel/time optimal problem has a singularity interval if

$$B^T\lambda(t) = \pm\alpha \qquad \forall t \in [t_1, t_2] \tag{A1}$$

This also implies that the kth derivative of Eq. (A1) is zero:

$$\frac{d^k}{dt^k}[B^T\lambda(t)] = 0 \qquad k = 1, 2, \ldots \tag{A2}$$

Substituting the solution of the costate equation

$$\lambda(t) = \exp(-A^T t)\lambda(0) \tag{A3}$$

and its derivatives into Eq. (A2), we require the following equation to be satisfied for a singularity interval to exist:

$$[B \quad AB \quad A^2B \quad A^3B]A^T\exp(-A^T t)\lambda(0) = 0 \qquad \forall t \in [t_1, t_2] \tag{A4}$$

Thus, singularities can exist if the system is uncontrollable or if the A matrix is singular. Since the floating oscillator is a controllable system and the A matrix is singular, there exists a possibility of a singular interval.

The state-space system can be transformed into the canonical form

$$\dot{x} = Ax + Bu \tag{A5}$$

where

$$A = \begin{bmatrix} 0 & 1 & 0 & 0 \\ 0 & 0 & 1 & 0 \\ 0 & 0 & 0 & 1 \\ 0 & 0 & -\omega^2 & 0 \end{bmatrix}, \qquad B = \begin{bmatrix} 0 \\ 0 \\ 0 \\ 1 \end{bmatrix} \tag{A6}$$

and the costate equation is

$$\begin{bmatrix} \dot{\lambda}_1 \\ \dot{\lambda}_2 \\ \dot{\lambda}_3 \\ \dot{\lambda}_4 \end{bmatrix} = \begin{bmatrix} 0 & 0 & 0 & 0 \\ -1 & 0 & 0 & 0 \\ 0 & -1 & 0 & \omega^2 \\ 0 & 0 & -1 & 0 \end{bmatrix} \begin{bmatrix} \lambda_1 \\ \lambda_2 \\ \lambda_3 \\ \lambda_4 \end{bmatrix} \tag{A7}$$

From Eqs. (A1) and (A7), we have

$$\begin{bmatrix} \lambda_1 \\ \lambda_2 \\ \lambda_3 \\ \lambda_4 \end{bmatrix} = \begin{bmatrix} 0 \\ \pm\alpha\omega^2 \\ 0 \\ \pm\alpha \end{bmatrix} \tag{A8}$$

One of the necessary conditions for optimality is

$$H(x, \lambda, u) = 1 + \alpha|u| + \lambda^T(Ax + Bu) = 0 \qquad \forall t \in [0, t_f] \tag{A9}$$

which in the singular interval can be represented as

$$H(x, \lambda, u) = 1 + \lambda^T Ax = 0 \qquad \forall t \in [t_1, t_2] \tag{A10}$$

which leads to the equation

$$\pm\alpha \begin{bmatrix} 0 & \omega^2 & 0 & 1 \end{bmatrix} \begin{bmatrix} 0 & 1 & 0 & 0 \\ 0 & 0 & 1 & 0 \\ 0 & 0 & 0 & 1 \\ 0 & 0 & -\omega^2 & 0 \end{bmatrix} \begin{bmatrix} x_1 \\ x_2 \\ x_3 \\ x_4 \end{bmatrix} = -1 \tag{A11}$$

which requires $0 = -1$. Thus, we have shown that the necessary condition for optimality conflicts with the condition for the existence of singular intervals, thus, precluding the existence of singular intervals.

The following development proves that the switching function for the benchmark floating oscillator is zero at midmaneuver time for a rest-to-rest maneuver.

It can be shown that the rigid-body displacement of the decoupled equations of motion at midmaneuver time is

$$\theta(T_2) = \tfrac{1}{2}\theta_f \tag{A12}$$

and the displacement of the flexible mode at time T_2 is

$$q(T_2) = 0 \tag{A13}$$

We now consider the separate optimal control problem with zero initial states and final states given by

$$\boldsymbol{x}(T_2) = \left[\tfrac{1}{2}\theta_f \quad \dot{\theta}(T_2) \quad 0 \quad \dot{q}(T_2)\right]^T \tag{A14}$$

which minimizes the cost function

$$J = \int_0^{T_2} (1 + \alpha|u_m|)\, \mathrm{d}t \tag{A15}$$

where the subscript m refers to the modified problem. Since the displacement states are fixed and the corresponding velocity states are free, the transversality condition requires

$$\boldsymbol{\lambda}(T_2) = [\lambda_1(T_2) \quad 0 \quad \lambda_3(T_2) \quad 0]^T \tag{A16}$$

Since the boundary conditions for this new optimal control problem match the corresponding states for the original problem, we have

$$u_m^*(t) = u^*(t) \qquad 0 < t < T_2 \tag{A17}$$

where the asterisk indicates optimal control. The switching function for the system represented by Eqs. (48–50) is given by the equation

$$B^T\boldsymbol{\lambda} = [0 \quad \phi_0 \quad 0 \quad \phi_1] \begin{bmatrix} \lambda_1(t) \\ \lambda_2(t) \\ \lambda_3(t) \\ \lambda_4(t) \end{bmatrix} = \lambda_2(t)\phi_0 + \lambda_4(t)\phi_1 \tag{A18}$$

Since

$$\lambda_2(T_2) = \lambda_4(T_2) = 0 \tag{A19}$$

the switching function is zero at the midmaneuver time.

Acknowledgment

The author gratefully acknowledges helpful discussions with S. R. Vadali.

References

[1]Singh, G., Kabamba, P. T., and McClamroch, N. H., "Planar Time-Optimal Control, Rest-to-Rest Slewing of Flexible Spacecraft," *Journal of Guidance, Control, and Dynamics*, Vol. 12, No. 1, 1989, pp. 71–81.

[2]Singh, T., and Vadali, S. R., "Robust Time-Optimal Control: Frequency Domain Approach," *Journal of Guidance, Control, and Dynamics*, Vol. 17, No. 2, 1994, pp. 346–353.

[3]Liu, Q., and Wie, B., "Robust Time-Optimal Control of Uncertain Flexible Spacecraft," *Journal of Guidance, Control, and Dynamics*, Vol. 15, No. 3, 1992, pp. 597–604.

[4]Ben-Asher, J., Burns, J. A., and Cliff, E. M., "Time-Optimal Slewing of Flexible Spacecraft," *Journal of Guidance, Control, and Dynamics*, Vol. 15, No. 2, 1992, pp. 360–367.

[5]Cannon, R. H., Jr., and Schmitz, E., "Initial Experiments on the End-Point Control of Flexible One-Link Robot," *International Journal of Robotics Research*, Vol. 3, No. 3, 1984, pp. 62–75.

[6]Redmond, J., and Silverberg, L., "Fuel Consumption in Optimal Control," *Journal of Guidance, Control, and Dynamics*, Vol. 15, No. 2, 1992, pp. 424–430.

[7]Farrenkopf, R. L., "Optimal Open-Loop Maneuver Profiles for Flexible Spacecraft," *Journal of Guidance, Control, and Dynamics*, Vol. 2, No. 6, 1979, pp. 491–498.

[8]Swigert, C. J., "Shaped Torque Techniques," *Journal of Guidance, Control, and Dynamics*, Vol. 3, No. 5, 1980, pp. 460–467.

[9]Vander Velde, W. E., and He, J., "Design of Space Structure Control Systems Using On-Off Control," *Journal of Guidance, Control, and Dynamics*, Vol. 6, No. 1, 1983, pp. 53–60.

[10]Lopes de Oliveira e Souza, M., "Exactly Solving the Weighted Time/Fuel Optimal Control of an Undamped Harmonic Oscillator," *Journal of Guidance, Control, and Dynamics*, Vol. 11, No. 6, 1988, pp. 488–494.

[11]Wie, B., and Bernstein, D. S., "Benchmark Problems for Robust Control Design," *Journal of Guidance, Control, and Dynamics*, Vol. 15, No. 5, 1992, pp. 1057–1059.